



Published in final edited form as:

Lab Chip. ; 21(18): 3458–3470. doi:10.1039/d1lc00598g.

***In Vitro* Assay for Single-cell Characterization of Impaired Deformability in Red Blood Cells under Recurrent Episodes of Hypoxia**

Yuhao Qiang^{a,b}, Jia Liu^a, Ming Dao^{*,b}, E. Du^{*,a}

^aOcean and Mechanical Engineering, Florida Atlantic University, 777 Glades Rd., Boca Raton, Florida, USA

^bDepartment of Materials Science and Engineering, Massachusetts Institute of Technology, 77 Massachusetts Ave, Cambridge, Massachusetts, USA

Abstract

Red blood cells (RBCs) are subjected to recurrent changes in shear stress and oxygen tension during blood circulation. The cyclic shear stress has been identified as an important factor that alone can weaken cell mechanical deformability. The effects of cyclic hypoxia on cellular biomechanics have yet to be fully investigated. As the oxygen affinity of hemoglobin plays a key role in the biological function and mechanical performance of RBCs, the repeated transitions of hemoglobin between its R (high oxygen tension) and T (low oxygen tension) states may impact their mechanical behavior. The present study focuses on developing a novel microfluidics-based assay for characterization of the effect of cyclic hypoxia on cell biomechanics. The capability of this assay is demonstrated by a longitudinal study of individual RBCs in health and sickle cell disease subjected to cyclic hypoxia conditions of various durations and levels of low oxygen tension. Viscoelastic properties of cell membranes are extracted from tensile stretching and relaxation processes of RBCs induced by the electrodeformation technique. Results demonstrate that cyclic hypoxia alone can significantly reduce cell deformability, similar to the fatigue damage accumulated through cyclic mechanical loading. RBCs affected by sickle cell disease are less deformable (significantly higher membrane shear modulus and viscosity) than normal RBCs. The fatigue resistance of sickle RBCs to the cyclic hypoxia challenge is significantly inferior to normal RBCs, and this trend is more significant in mature erythrocytes of sickle cells. When oxygen affinity of sickle hemoglobin is enhanced by anti-sickling drug treatment of 5-hydroxymethyl-2-furfural (5-HMF), sickle RBCs show ameliorated resistance to fatigue damage induced by cyclic hypoxia. These results illustrate that an important biophysical mechanism underlying RBC senescence in which cyclic hypoxia challenge alone can lead to mechanical degradation of the RBC membrane. We envision the application of this assay can be further extended to RBCs in other blood diseases and other cell types.

*corresponding authors: mingdao@mit.edu (M.D.) or edu@fau.edu (E.D.).

Conflicts of interest

There are no conflicts to declare.

Introduction

Hypoxia, a low oxygen tension condition, is a very common microenvironmental factor in physiological processes of blood circulation and varied pathological processes, such as cancer, chronic inflammation, myocardial infarction, stroke and ischaemic acute kidney injury.^{1, 2} Red blood cell (RBCs) are the most abundant cells in blood, serving as the O₂ carriers in human body. In blood circulation, RBCs repetitively encounter various oxygen tension levels, which can be as high as 10–13% O₂ in arteries, lung alveoli and liver,³ or as low as 5% O₂ in venous blood, 0.5–7% O₂ in bone marrow and brain, and down to 1% O₂ in cartilage.⁴ They are strongly influenced by the surrounding oxygen tension in the autonomous regulation of their own properties and physiological functions.⁵ RBCs produce reactive oxygen species by the oxidation of ferric (Fe³⁺) to ferrous (Fe²⁺) iron in the heme complex, which can be offset by the systemic antioxidant defense mechanisms. The imbalance between these two processes, known as oxidative stress, can affect cellular membrane lipids and proteins, leading to impaired membrane, cellular deformability, senescence,^{6–8} as well as abnormal aggregation and adhesion kinetics.^{9–11} Interplay between poor cellular deformability and impaired oxygen delivery is observed in various pathological processes, such as sickle cell disease.¹² RBCs affected by sickle cell disease are prone to the influences of the oxygen tension variation due to a mutation in the hemoglobin gene, leading to hemoglobin polymerization under hypoxia and the associated membrane abnormalities.⁵ Prior studies have demonstrated that sickle RBCs exhibit compromised deformability compared to normal RBCs, which becomes even worse upon deoxygenation.^{13–15} Moreover, repeated sickling-unsickling processes in response to the cyclic hypoxia challenge were reported to lead to progressive reduction in sickle RBC deformability even after reoxygenation.^{16, 17} These studies have advanced our understandings of the interactions between hypoxia and cell biomechanics, as well as the underlying mechanisms of the accelerated damage in diseased RBCs. However, the exact mechanism underlying the RBC senescence remains to be fully elucidated.

Mechanical degradation of RBCs has been generally deemed as a main cause of RBC membrane failure during *in-vivo* and extracorporeal circulation. One factor that could be responsible for the RBC mechanical degradation is the cumulative fatigue damage from the cyclic shear stresses.¹⁸ The cyclic tensile stretching-relaxation loading alone can lead to mechanical fatigue of RBCs *in vitro*.^{18, 19} Additionally, as circulating RBCs experience cyclic changes in oxygen tension, the accumulated oxidative damage may also take part in the degradation process of cell biomechanics, along with shear stresses. Two biological processes in cell membranes are likely initiated and cumulated, along with the cyclic hypoxia process, including recurrent oxidative stress and alterations in cytoskeleton by damaging the spectrin network of cell membranes, contributing to the impaired RBC deformability and biomechanics.²⁰ This is similar to the scenario that membrane nano-structural alterations occur due to chemically induced oxidative stress.²¹ Another possible biological process associated with the deoxygenation process is the adenosine triphosphate (ATP) release, following the parallel effects of IgG/ band 3/ Heinz body co-clustering, increased intracellular calcium ions, glycolysis, G_i protein activation and so forth.^{14, 22} Collective evidences have shown that ion transport and kinase-regulated

phosphorylation are two central mechanisms of implicating RBC deformability due to the disruption of stability of interaction between cytoskeletal proteins and membrane complexes.^{23, 24} Increased intracellular calcium ions (Ca^{2+}), for instance, has long been known as a factor that leads to impairment of RBC deformability, which is regulated by Ca^{2+} -ATPase activity under exposure to shear stress and hypoxic conditions.^{25, 26} A recent study has investigated the effects of two kinases Lyn and GSK3 α on regulating the capability of RBCs to undergo repeated mechanical deformations.²⁷ The selected kinases Lyn and GSK3 α are known regulators of the cytoskeleton-interacting proteins band 3 and β -adducin, respectively.^{28, 29} Decrease in the microcapillary traversal velocity in RBCs was generally observed after treatment with both Lyn inhibitor (Bafetinib) and GSK3 inhibitor (CHIR-98014). Inhibition of these two kinases was found resulting in the inability of RBCs to recover from successive deformations. To our knowledge, in addition to mechanical stimulus, deoxygenation could also possibly induce oxidative phosphorylation of RBC proteins and subsequent modification of cytoskeletal structures.^{30, 31} Thus, we are proposing a biophysical mechanism underlying the RBC senescence in which cyclic hypoxia causes mechanical degradation in cell membranes, as analogous to the process of membrane mechanical fatigue from cyclic shear stresses. This requires a strategy to subject RBCs to well-controlled repeated hypoxia microenvironment while allowing simultaneous characterization of cell mechanical properties. Early studies of RBC deformability under hypoxia were mostly carried out after incubating cells in a closed hypoxic chamber for a long duration.^{9, 17, 32, 33} It is therefore hard to replicate the cyclic variations in oxygen tension as circulating RBCs experience *in vivo* while simultaneously measuring the biomechanical properties of RBCs under repeated transient hypoxia. Microfluidics serves as a miniaturized and efficient platform for gas diffusion by interfacing the gas and aqueous solution through flow or a gas-permeable membrane,^{34, 35} which is also amenable to the control of cellular gaseous microenvironment.^{4, 36} A few previous studies have demonstrated successful applications of such microfluidic hypoxia assays in the cell morphological study.^{37–39} Integrated microfluidic approaches have also been developed to control the oxygen tension on cells and simultaneously measure their biomechanical properties. For example, Zheng et al developed a microfluidic approach to study the mechanical properties of RBCs under deoxygenated conditions.⁴⁰ Similar methods were reported to characterize cell velocity or occlusion index under deoxygenation.^{41–43} However, these existing methods are limited to measurements of the averaged behavior of a cell population, and not suitable for the longitudinal study of individual RBCs.⁴⁴ A variety of other methods that can successfully measure the deformability of RBCs at single cell level,⁴⁵ such as micropipette aspiration³³ and optical tweezers⁴⁶, but are difficult to be equipped with cellular gas microenvironment control. In addition, these single-cell measurement techniques are limited by their inherent low throughput.

In this work, we develop a novel *in vitro* assay for cell deformability measurement under well-controlled cyclic hypoxia, by integrating electrodeformation technique into a microdiffusion chamber. This method is advantageous in its ease of implementation and flexibility in simultaneous application of repeated hypoxia challenge and shear stresses on individual cells in suspension and in quasi-stationary conditions. To determine whether cyclic hypoxia challenge alone can lead to fatigue degradation in cell membranes, we

measure cellular viscoelastic behavior and characterize the progressive change in membrane shear modulus and viscosity along with various loading histories in normal RBCs. Molecular mechanisms relevant to the cyclic hypoxia-induced fatigue of RBCs is partially investigated by characterization of intracellular Ca^{2+} and inhibition of Piezo 1 channels as well as two phosphorylase kinases (Lyn and GSK3 α). We then test the possible expedited fatigue of RBCs affected by sickle cell disease, and the effects of anti-sickling agent 5-hydroxymethyl-2-furfural (5-HMF) on the mechanical performance of sickle RBCs that are subjected to cyclic hypoxia challenge.

Materials and methods

Sample preparation

Healthy blood samples were obtained with verbal consent of the two donors, following Institutional Review Board (IRB) approval from Florida Atlantic University. Sickle cell samples were obtained with informed consent from patients with sickle cell disease during their clinic visits at the University of Miami following the IRB approval; additional sickle cell samples were collected under an Excess Human Material Protocol approved by the Partners Healthcare Institutional Review Board with a waiver of consent. More sample information can be found in Table S1 in SI Appendix, *Detailed information of sickle cell samples*. All samples were stored at 4 °C and tested within one week of collection. The working buffer for biomechanics measurement was prepared by mixing 8.5% (w/v) sucrose and 0.3% (w/v) dextrose in deionized water, and further adjusting the electrical conductivity to 0.15 S/m using phosphate buffered saline (PBS) solution (Lonza Walkersville, Inc., Walkersville, MD). The pH was adjusted to 7.4 with NaOH/HCl. The osmolality of the working buffer was measured to be ~290 mOsm/kg using an osmometer (Advanced Instruments, Inc., MA, US). Prior to each experiment, blood samples were washed twice with PBS at the speed of 2000 rpm at room temperature for two minutes. The hematocrit of each tested sample was adjusted to be 0.1% by resuspending 1 μL RBC pellet into 1 mL of working buffer. To investigate the effect of 5-HMF on mechanical performance of RBCs that are subjected to cyclic hypoxia, RBCs were incubated with 5-HMF (5 mM) for 60 min at 37 °C in Eppendorf tubes. The treated cells were washed twice with PBS to remove residual 5-HMF, and then resuspended into the working buffer for measurement. The non-treated RBC suspensions were used as control group. Sickle cell fractionation was performed by means of a three-step discontinuous gradient, which was stacked by four layers of 2 mL gradient solutions of densities 1.077, 1.092, 1.095 and 1.100 g/mL, respectively. The gradient solutions were prepared following the manufacturer's protocol (OptiPrep™ Application Sheet C35: available at <https://www.axis-shield-density-gradient-media.com/C35.pdf>). A 2 mL of blood sample was washed twice with PBS at 2000 rpm for 5 min, and then the RBC pellet was fully suspended by a gentle vortex and layered on top of the density gradient. Cell fractionation was achieved by centrifugation at 1000 \times g at 21 °C for 30 min. The reticulocyte-enriched and erythrocyte-rich cell subpopulations respectively trapped in the 2nd and 4th interfaces of stacked layers of gradient solution were carefully collected using a 1-mL pipette tip and washed with 5 mL PBS buffer twice to remove gradient solution residue. Fractionated sickle RBCs were then resuspended in PBS containing 1% (w/v) BSA (Sigma-Aldrich) and stored at 4 °C shortly before experiment. The reticulocyte yield of

each cell subpopulation was measured by counting reticulocytes identified with supravital staining using new methylene blue.⁴⁷

Experimental setup

Fig. 1A provides a schematic of the complete experimental system. To study the tendency of change in the mechanical properties of RBCs, the viscoelastic properties of RBCs were measured at the initial, intermediate and end time points and presented at equivalent cycles during the cyclic hypoxia process. Fig. 1B shows the sequence diagram of serial mechanical testing of RBCs performed at the selected time points during the challenge of repeated Deoxygenation-Oxygenation (DeOxy-Oxy) cycles. The microfluidic chip consists of a polydimethylsiloxane (PDMS) double-layer microchannel and two gold thin-film interdigitated electrode arrays (IEAs) coated on a 0.7 mm thick glass substrate (Fig. 1B and C). Both the upper gas channel and the lower cell channel are 1500 μm wide and 150 μm deep. The two channels are aligned perpendicular to each other and separated by a 150 μm thick gas permeable PDMS film in the intersectional area. The change of osmolality due to the loss of water across the PDMS membrane was found negligible within 1 hour of experiment.⁴⁸ The IEA consists of 16 pairs of fingers with 20 μm band and 20 μm gap. The PDMS microchannel was fabricated by casting a SU-8/Si mold with a degassed PDMS mixture of base and curing agent (10:1, w/w) at 70°C for 2 hours. The SU-8/ Si mold and IEA were fabricated following standard microfabrication techniques as introduced previously.⁴⁹ Permanent covalent bonding was created between the two PDMS layers and the IEA glass substrate following a 60-second air plasma treatment in a plasma cleaner (Model PDC-001, Harrick Plasma). The cell channel was loaded with cell suspension by injection with a 1 mL syringe, and the gas channel was connected to gas supplies via tygon tubing at the regulated pressure. A programmable 3-way valve (LabSmith., CA, USA) was used to switch between these two gas supplies of different gas mixtures, including an oxygen rich gas mixture (133 mmHg): 17.5% oxygen, 5% carbon dioxide with the balance of nitrogen, and an intermediate oxygen gas mixture (38 mmHg): 5% oxygen, 5% carbon dioxide with the balance of nitrogen or an oxygen poor gas mixture (0 mmHg): 5% carbon dioxide with the balance of nitrogen. The IEA electrode pads were soldered to copper-based wires, allowing electrical excitation from a function generator (SIGLENT SDG830, SIGLENT, P.R. China) to produce dielectrophoresis (DEP) and electrodeformation of cells (Fig. 1D). Cell behavior was observed via a high-resolution CMOS camera (The Imaging Source, Charlotte, NC) which is mounted on an Olympus X81 inverted microscope (Olympus America, PA, USA), with image contrast being enhanced by inserting a 414 ± 46 nm band pass filter in the optical path.

RBC mechanical measurement

Mechanical properties of RBCs were characterized from their viscoelastic response to a fixed loading condition, which was implemented using a constant-amplitude electrodeformation strategy. The mechanical measurement was performed in the hydrostatic condition once the suspended cells settled down to the IEA glass substrate in the microchannel due to gravity. By tuning the frequency of applied electrical signal, cells moved toward the electrode edges due to under positive DEP and were gradually stretched into a quasi-ellipsoid shape due to electrodeformation; Upon the applied electrical voltage

turned off, cells gradually relaxed to their original shape. The root mean square values of the supplied voltage was 3 V at 1.58 MHz for 2 s and 0 V for 2 s, respectively. The corresponding shear stress (σ) exerted on RBCs was 2.85 Pa and 0 Pa as calibrated in our previous work.¹⁸ Deformability measurements were conducted by subjecting cells to repeated constant-amplitude electrodeformation loading for 5 continuous cycles (recorded at 40 frames per second). The viscoelastic properties of RBCs were then averaged from these 5 cycles for each individual cell. To prevent the interferences of HbS polymerization on cell deformability, mechanical testing was performed under oxygenated condition for both normal and sickle RBCs. Cell deformation was quantified by the transient extension ratio $\lambda(t)$, defined as the instantaneous value of the contraction ratio $b_{t=0}/b(t)$ in the transverse direction of tensile loading (Fig. 2A). Considering the less accuracy of the long axis a measured along the tensile loading direction as a small part of the deformed cell membrane is blocked from view by the IEA, axial extension ratio $\lambda'(t)(=a(t)/a_{t=0})$ was converted by $1/\lambda(t)$ on the assumption that the total membrane area of cell is a constant during deformation, following the protocol validated in our earlier study.¹⁸ Values of $\lambda(t)$ during the stretching phase and the relaxation phase in each cycle can be fitted well with the Kelvin-Voigt solid model.⁵⁰ In present study, mechanical properties of cells were evaluated by the values of membrane shear modulus (μ) and shear viscosity (η) thereby extracted from the tensile stretching-relaxation profile accordingly. More details of electrodeformation characterization and constitutive model of viscoelastic deformation of RBCs can be found elsewhere.^{18, 19, 51}

Fluo-4 imaging of calcium in RBCs

Isolated RBCs were washed three times with PBS, and then loaded with 1mM Fluo-4 AM (Thermo Fisher Scientific, Waltham, USA), a fluorescent probe suitable to assess intracellular calcium-levels in living RBCs.⁵² Cells were incubated with Fluo-4 AM for 60 min at room temperature and shielded from light, and then washed three times with PBS before the DeOxy-Oxy experiment. Fluo-4-loaded RBCs were excited at wavelength $\lambda = 488$ nm and the fluorescent signal was captured at $\lambda = 505$ nm using the inverted microscope as forementioned. The fluorescence of cells in the same field of view was recorded during the DeOxy-Oxy experiment and the fluorescent intensity was determined using Image J (National Institutes of Health, Bethesda, USA). To be noted, intracellular Ca^{2+} content of RBCs was determined by the Fluo-4-emitted fluorescent intensity (F) relative to the baseline (F0, the value measured at $t=0$ in the oxygenated state), which just provides the change of intracellular Ca^{2+} over time.

Inhibition of RBC signaling pathways

GsMTx4 is known as a spider venom peptide that can selectively inhibit cationic mechanosensitive channels, such as Piezo channel families.⁵³ Thus, for inhibition of RBC stretch-activated mechanosensitive channel, RBCs were pretreated with GsMTx4 (1 μM , Abcam, Cambridge, USA) for 30min. In addition, for inhibition of Lyn and GSK3 α kinases, cells were pretreated with 3 μM Bafetinib (Cat. No. 50-187-3889, Fisher Scientific) and 10nM GSK3 inhibitor CHIR-98014 (Cat. No. 66-955, Fisher Scientific) for 1 min at 37 °C. Selections of these two specific kinases inhibitors were referred to a previous study.²⁷ Due to the fact that all the inhibitors used in the experiments are dissolved in dimethyl sulfoxide

(DMSO) for stock solutions, cells were treated with DMSO of equivalent concentration in the inhibitors as a control.

Statistical Study

Data was analyzed using GraphPad software (GraphPad Software, Inc., La Jolla, CA, USA). All data were expressed in terms of statistical mean \pm SEM unless otherwise specified. Outliers were identified and excluded from the analysis using ROUT method with GraphPad software. A paired t-test was used to determine p values between different measurements of same cell population. A two-sample t-test was used to generate the p values between measurements for different cell populations. One-way ANOVA test was used to compare measurements of same cell population over the loading cycles. * $p < 0.05$ was considered as statistically significant.

Results

Effect of static oxygen tension on RBC deformability

A unique feature of our system lies in that the cell deformability measurement can be made on multiple, individually tracked RBCs under a well-controlled oxygen tension environment. Cell deformability of RBCs in the oxygenated and deoxygenated states were characterized under the same electrodeformation loading. It is likely that differences exist in the dielectric properties of subcellular components in RBCs between the R (oxygenated) and T (deoxygenated) states of hemoglobin, leading to variations in the actual shear forces exerted on cell membranes and eventually the extension ratio and the viscoelastic characterization. Notwithstanding, considering the variation in the electrodeformation force is comparatively small according to the parametric analysis in our previous study,¹⁸ the viscoelastic characteristics of cells under each condition were obtained based on the same dielectric properties of normal RBCs.⁵⁴

The effect of oxygen tension on cell deformability was obtained by comparing the values of λ and viscoelastic characteristics for each cell in fully deoxygenated state for 2 min to the control values in fully oxygenated state for 2 min, respectively. Figs. 2A and B show the instantaneous value of λ as function of time measured within five consecutive cycles for oxygenated and deoxygenated normal (AA) RBCs, respectively. Cells show typical viscoelastic behavior in each cycle regardless of oxygen state of intracellular hemoglobin, which can be fitted to the Kelvin-Voigt model as shown in Fig. 2C. Figs. 2D and E show the scatter plot of μ and η values of individually characterized AA RBCs under the static oxygenated and deoxygenated states, respectively. Both μ and η values show significant overlap among the consecutive cycles, indicating negligible influence on RBC mechanical properties from a few (5) cycles of electrodeformation under both normoxia and hypoxia. The mean values of μ and η for AA RBCs measured in oxygenated state are consistent with those reported in previous studies^{50, 55}. Effect of hypoxia on cell deformability was found to be significant in AA RBCs ($p < 0.001$). Mean values of μ increased from $2.93 \pm 0.15 \mu\text{N/m}$ to $3.54 \pm 0.13 \mu\text{N/m}$; values of η increased from $0.44 \pm 0.03 \mu\text{N/m}\cdot\text{s}$ to $0.50 \pm 0.04 \mu\text{N/m}\cdot\text{s}$ in AA RBCs ($n = 49$) after deoxygenation. We found cells were less deformable at the very low oxygen tension, which was also reported previously.^{10, 11}

Additionally, in order to investigate the effect of long-term hypoxia on cell deformability, we measured the progression of μ and η values for AA RBCs in oxygenated state and deoxygenated state lasting for 60 min (Figs. 2 F – I). Mechanical tests were performed when cells were fully reoxygenated at the time points of 0, 30 min and 60 min, respectively. Values of μ and η show no significant changes under the static oxygenated state within 60 min ($p > 0.05$), indicating that under the normoxia environment (with only a few cycles of electrodeformation in-between for mechanical property evaluation) results in no detectable influence on the RBC deformability in our experiment. In contrast, both μ and η show continuous increases after 30 min and 60 min of prolonged static deoxygenation ($p < 0.0001$). These results demonstrated the impairment in cell deformability was exacerbated in a cumulative manner versus total deoxygenation time under the static deoxygenated state on RBCs.

RBC mechanical degradation induced by cyclic hypoxia

To further investigate the effect of variation in cyclic hypoxia simulating the complexity of *in vivo* hypoxia cycling, we measured the mechanical degradation of RBCs subjected to various hypoxia cycling conditions. We varied the time duration of deoxygenation in each cycle to 30 s, 60 s, 90 s and 120 s, respectively. The corresponding in-situ values of dissolved O₂ concentration in the cell channel were pre-calibrated by a FireStingO2 fiber-optic oxygen microsensor (Pyro Science™, Aachen, German), see SI and Figs. S1 and S2 for details. The O₂ concentration in the system reached equilibrium between the cell channel and the gas channel within 15 s. Oxygenation time was set as 30 s in each cycle, allowing cells to be fully reoxygenated. The extent of cellular stiffening in association with hypoxia cycling was characterized by the progression of maximum extension ratio λ_{\max} along with hypoxia cycles as well as cumulative deoxygenation time, as are summarized in Tables S2 and S3, respectively. The results showed that the reduction rate in λ_{\max} increased with the number of hypoxia cycles. Within a same cumulative deoxygenation time, e.g., 30 min, the decrease in λ_{\max} under the DeOxy-Oxy condition of 30 s-30 s was much higher than that under the DeOxy-Oxy condition of 120 s-30 s (10.68% vs 5.48%). On the other hand, it was found that the reduction rate in λ_{\max} increased with the increase of hypoxia duration in each cycle: a decrease of 4.46% for the DeOxy-Oxy condition of 30 s-30 s as compared to a decrease of 7.92% for the DeOxy-Oxy condition of 120 s-30 s, within the same 24 cycles of hypoxia. Taken together, the hypoxia-induced stiffening in RBCs is determined by the cumulative time of deoxygenation as well as the total number of hypoxia cycles. This suggests that the cyclic hypoxia may constitute another key factor comparable to the cyclic shear stresses, and both factors contribute significantly to the mechanical degradation of RBCs during microcirculation.

Cyclic-hypoxia-induced RBC mechanical degradation under severe and mild deoxygenation cycles

To assess the influences of the severe and mild deoxygenation conditions on the cyclic-hypoxia-induced cell deformability reduction, we investigated two levels of hypoxia: 0% O₂ and 5% O₂, while retaining the same level of oxygen tension for the oxygenated condition (17.5% O₂). Figs. 3A and B show the comparisons of μ and η values measured from the same individual RBCs, before and after the deoxygenation processes in the initial

DeOxy cycle of these two respective conditions. In contrast to the drastic impairment of deformability (28.4 % increase in μ and 27.6 % increase in η) under the severe deoxygenation condition (17.5% O₂ - 0% O₂), changes of these two mechanical parameters are very small (0.72 % decrease in μ and 0.04 % increase in η) under the mild deoxygenation condition (17.5% O₂ - 5% O₂). The cumulative deformability changes under the cyclic DeOxy-Oxy (120s-30s) of these two different oxygen tension levels are shown in Figs. 3C and D). We found the rate of increases in μ and η values under the cycling of 17.5% O₂ - 0% O₂ (45.6 % increase in μ and 33.5 % increase in η after 60 min) are higher than those under the cycling of 17.5% O₂ - 5% O₂ (27.3 % increase in μ and 31.0 % increase in η after 60 min). These results suggest that cyclic-hypoxia-induced RBC mechanical degradation under the severe deoxygenation condition is much higher compared to those under the mild deoxygenation condition.

Exploring possible molecular pathways associated with cyclic-hypoxia-induced RBC mechanical degradation

To further explore the possible underlying molecular mechanisms associated with the cyclic hypoxia-induced mechanical degradation in cell membranes, we investigated a couple of known signaling pathways on RBCs. We especially examined the differences between non-cyclic hypoxia vs cyclic hypoxia and documented any cumulative effect vs hypoxia cycles.

We characterized the progression of intracellular Ca²⁺ content of RBCs under cyclic loadings of DeOxy-Oxy (120s-30s). Fig. 4A shows the representative fluorescent images obtained from individual RBCs loaded with the calcium-sensitive dye Fluo-4 over time in the oxygenated and deoxygenated states, respectively. The change of intracellular Ca²⁺ content of RBCs, determined by the Fluo-4-emitted fluorescent intensity (F) relative to the baseline (F_0 , the value measured at $t = 0$ in the oxygenated state), is presented in Fig. 4B. Value of F/F_0 showed 20% increase in the deoxygenated state relative to the baseline in the initial cycle of DeOxy-Oxy, and showed sustained elevations in the deoxygenated state after cyclic hypoxia (52% increase after 30 min or 12 cycles, and up to 70% increase after 60 min or 24 cycles). This result is aligned with the observation in earlier studies.^{26, 56} It is noteworthy that, even measured in the oxygenated state, we also found elevation of intracellular Ca²⁺ content in RBCs after cyclic hypoxia (21% increase after 30 min or 12 cycles, and up to 40% increase after 60 min or 24 cycles). This finding suggests that the deoxygenation-induced influx of Ca²⁺ in RBCs is *not fully reversible upon reoxygenation*, which may lead to the cumulative elevation of intracellular Ca²⁺ content of RBCs over multiple DeOxy-Oxy cycles.

Piezo 1 is the particular mechanosensitive cation channel expressed on RBC membranes that regulates stretch-induced ATP release in RBCs.⁵⁷ Therefore, in order to investigate whether cyclic-hypoxia-induced RBC mechanical degradation is linked to the stretch-induced activation of mechanosensitive cation channel, we inhibited Piezo 1 channels of RBCs using a mechanosensitive channel inhibitor GsMTx4. Figs. 4C and D compare the changes in μ and η values of RBCs between the GsMTx-4 treated cells and the control (DMSO treated cells) under the same cyclic loadings of DeOxy-Oxy (90s-30s) within 60 min. The results of GsMTx-4 incubated cells ($n = 92$) remained at the same level as with the control group

($p > 0.05$), indicating that hypoxia-induced mechanical degradation of RBCs may not be directly related to Piezo 1 mechanosensitive channels. In this regard, alternative signaling mechanisms would require further investigation.

In addition to activity of ion transport, kinase-regulated phosphorylation is also known to be involved in RBC stiffening. Thus, the effects of inhibiting two kinases (Lyn and GSK3 α) on the hypoxia-induced mechanical degradation of healthy RBCs were investigated. Figs. 4E and F show the comparison of progression in μ and η values of Lyn inhibited cells ($n = 91$), GSK3 inhibited cells ($n = 83$) and the control ($n = 77$) under the same cyclic loadings of DeOxy-Oxy (90s-30s). The inhibition of Lyn kinase by Bafetinib showed very small or nonsignificant effect on the RBC deformability degradation (change in μ) compared to the control samples under normoxia (cycle 0) or after multiple DeOxy-Oxy cycles, confirming that phosphorylation of band 3 does not directly affect RBC mechanical stability, which is consistent with earlier studies that performed under normoxia after repeated mechanical stress.^{27, 58} Notably, the inhibition of GSK3 kinase by CHIR-98014 demonstrated significant RBC mechanical degradation (increase in μ) compared to the control samples under normoxia (cycle 0) and after multiple DeOxy-Oxy cycles, which is consistent with an earlier study (performed only under normoxia) that phosphorylation of β -adducin mediated by GSK3 kinase affects its interactions with the spectrin-actin cytoskeleton and consequently influences RBC deformability.²⁹ Compared with the control sample (without adding any kinase inhibitor), the impact of adding the inhibitor CHIR-98014 changes with the accumulated number of hypoxia cycles. Therefore, through investigating the impact of inhibiting part of these signaling pathways, we can speculate that RBC deformability could be vulnerable to the cumulative disruption of enzyme activities involved in the DeOxy-Oxy process, although more studies are needed to figure out more details and any potential effective interventions.

Effect of cyclic hypoxia on RBCs in sickle cell disease (SCD) patients

To investigate the effects of cyclic hypoxia on cell deformability in diseased condition, we conducted a pilot study of measuring the deformability of sickle (SS) RBCs under both static and cyclic hypoxia conditions. Figs. 5A and B compare the averaged instantaneous value of λ of SS RBCs as a function of time measured within five consecutive mechanical loading cycles under the static oxygenated (17.5% O₂) and the static deoxygenated (0% O₂) conditions respectively. We again noted that a small number of serial mechanical cyclic loadings (used for evaluating mechanical properties) do not change the RBC mechanical properties, as shown by Figs. 5A–D. Figs. 5C and D show the extracted μ and η values of individually characterized SS RBCs ($n = 73$) in the static oxygenated and deoxygenated states, respectively. Compared to the results of AA RBCs (Figs. 2D and E), SS RBCs were found to be less deformable and more viscous in both oxygenation and deoxygenation states, with greater variations in both viscoelastic parameters, which agrees with the previous study.⁵⁹ SS RBCs also showed reduction in cell deformability due to deoxygenation, with mean value of μ increased from 4.39 ± 0.14 $\mu\text{N/m}$ to 5.46 ± 0.21 $\mu\text{N/m}$ after deoxygenation; values of η increased from 0.50 ± 0.02 $\mu\text{N/m s}$ to 0.75 ± 0.08 $\mu\text{N/m s}$ after deoxygenation. The measured mean values of μ and η for SS RBCs are consistent with those reported in the literature.^{40, 60} Notably, the averaged values of μ and η are significantly higher in SS

RBCs than AA RBCs (49.8% increase in μ and 13.6% increase in η for the oxygenated state vs 54.2% increase in μ and 50% increase in η for the deoxygenated state), consistent with observations reported in prior studies.^{61–63} This observation may be attributed to additional effect from the polymerization of deoxygenated HbS and its concurrently mutated interactions with cell membranes.⁵

Figs. 5E and F left panels show significant elevations in both μ and η for SS RBCs along with increasing DeOxy-Oxy cycles. Compared with the results of AA RBCs, similar increasing trend was found in SS RBCs but at much faster rate of elevation for shear modulus and viscosity (46.8% increase in μ and 37.1% increase in η for AA RBCs vs 98.7% increase in μ and 120.7% increase in η for SS RBCs after 60 min of treatment), which is likely attributed to additional factors contributed by the sickling-unsickling procedures of SS RBCs.¹⁶ We observed some cells behaved as hyper-rigid “solid-like” after only a few cycles of hypoxia. Furthermore, we carried out an additional experiment by selecting the subpopulation of SS RBCs that sickle under hypoxia (i.e. those show significant morphological changes/membrane crenation during the DeOxy-Oxy cycles), and found both μ and η values of these cells increased much faster than those of AA RBCs (Figs. S3). These results suggest that the effects of cyclic hypoxia on viscoelastic behavior of SS RBCs are also significant. Sickle RBCs are more vulnerable to cyclic-hypoxia induced mechanical degradation than normal healthy RBCs. We note that, previous studies of comparing sickle cells and normal cells in deformability mainly focused on the influence under a monotonical loading of deoxygenation, where the reduced cell deformability is essentially fully reversible when cells become reoxygenated. The current study enabled for the first time a demonstration of the key role of cyclic hypoxia resulting in cumulative mechanical property degradation of sickle cells, which may be a possible mechanism underlying the shortened lifespan of RBCs in SCD.

5-HMF is a common product from the reaction of reducing sugars and amino acids naturally occurring in foods, which has been reported to have anti-sickling effect on sickle cells by improving the oxygen affinity of hemoglobin.^{64–66} To further study whether the antioxidant 5-HMF can preserve RBC deformability after multiple DeOxy-Oxy cycles, we compared the shear modulus (μ) and shear viscosity (η) values between treated and non-treated AA and SS RBCs (Figs. 5E and F). The effect of 5-HMF treatment on the rate of elevations in shear modulus and viscosity along with the cyclic DeOxy-Oxy process were statically significant for both normal and sickle RBCs. Elevations in μ and η values are both remarkably smaller comparing with those of the non-treated groups (40.9% increase in μ and 17.2% increase in η for AA RBCs; 40.3% increase in μ and 77.1% increase in η for SS RBCs after 24 cycles of DeOxy-Oxy). These results indicate that improved oxygen affinity of hemoglobin can ameliorate and preserve deformability and mechanical performance of in both healthy and diseased RBCs. Therefore, our method can be potentially useful for in-vitro testing of treatment efficacy of many preclinical and early phase pharmacologic trials, such as GBT021601⁶⁷ and gene therapies.⁶⁸

In consideration that reticulocytes possibly have distinct mechanical performance under cyclic hypoxia due to their less mature membrane compared to mature erythrocytes, faster mechanical degradation found in sickle RBCs might also be attributed to the higher

percentage of reticulocytes (averaged 7.4% per CBC data for the tested SS-RBCs shown in Figs. 5E and F). In order to examine this possibility, we compared the change in deformability of RBCs taken from two more sickle cell patients between the reticulocyte-enriched (SS1, ~37% reticulocyte yield) and erythrocyte-rich (SS2, ~5% reticulocyte yield) cell subpopulations separated by different cell density fractions (Figs. 5G and H). Both μ and η values measured in SS1 (n = 70) and SS2 (n = 69) showed significant increase (62.6% increase in μ and 1.32 times increase in η for SS1; 60.1% increase in μ and 1.87 times increase in η for SS2 after 24 DeOxy-Oxy (120s-30s) cycles). We found the μ and η values measured from SS2 showed a faster increase compared to those measured from SS1, which suggests that less dense RBCs including the reticulocytes in SCD patients have higher resistance to cyclic-hypoxia-induced mechanical degradation compared to those more dense/mature erythrocytes in the blood taken from SCD patients. These results suggest that the faster mechanical degradation of sickle RBCs is not caused by their relatively higher percentage of reticulocytes. Additionally, as our results were measured from *a longitudinal study of individual RBCs*, we found the trend of mechanical degradation under cyclic hypoxia is highly consistent in most of the cells (~90%) regardless of the cell subpopulation from the reticulocyte-enriched group or the erythrocyte-rich group.

Discussion

RBC plays an important role in the regulation of microcirculatory blood flow in response to the variations of oxygen level *in vivo*. The accumulated evidence has shown that RBC capillary velocity elevates under hypoxic conditions.^{5, 69} The underlying mechanisms remain elusive and mainly center on two different explanations: (1) The elevated blood flow velocity is owing to the reduction of blood viscosity caused by the increase of RBC deformability under hypoxia; (2) Hypoxia-induced ATP release from RBCs stimulates the production of nitric oxide (NO) from vascular endothelial cells. And as a result, the produced NO subsequently activates the vasodilation, i.e., the relaxation of blood vessel, resulting in the acceleration of blood flow.⁷⁰ However, controversial results about the RBC deformability in response to deoxygenation have been reported in the relevant literature. Some prior studies have reported that RBC membrane becomes more rigid at low oxygen tension,^{10, 56} while some other studies found no significant alteration of deformability between oxygenated and deoxygenated RBCs.^{8, 11, 71} On the contrary, several recent studies have shown that RBC deformability increases under hypoxic conditions.^{41, 69, 72} The discrepant results from these studies may be mainly attributed to the differences in blood samples, deformability measurement techniques, and stability of experimental conditions such as temperature and oxygen control. Herein, our results demonstrated that deformability of RBC decreases under deoxygenation conditions by before-and-after mechanical characterization of individual cells in response to the switching of oxygen levels within a well-controlled microfluidic device. Therefore, we speculate that vasodilation led by the ATP release from RBCs might be the dominant cause of elevation in blood flow velocity under hypoxia.

Many factors coexist resulting in the functional degradation and senescence of RBCs, and the corresponding changes in mechanical or rheological properties have long been considered as important biomarkers. In particular, this work focuses on the effect

of cyclic hypoxia versus RBC mechanical degradation. It should be noted that the selection of severe DeOxy-Oxy condition in the present study was mainly based on our consideration of developing a microfluidic device for *in-vitro* quantitative characterization of expedited mechanical degradation under cyclic hypoxia; We sought to quickly see any significant changes in mechanical properties of RBCs within 60 min in our *in vitro* system, while minimizing other influencing factors, e.g., osmolality and metabolism. Our findings show that cyclic hypoxia challenge alone can gradually cause degradation in cell membrane biomechanics. This process in combination with the deformation-induced mechanical fatigue^{18, 19} represent two major fatigue loading conditions that circulating RBCs experience. Previous studies have provided the insights that mechanical deformation and deoxygenation are two major physiological stimuli of ATP release, resulting in the mechanical degradation of RBCs.^{70, 73} However, the relationship or discrepancy between these two stimuli still remain unclear. There is evidence that these two stimuli are essentially linked, in that deoxygenation could simultaneously promote the membrane fluctuations (a special type of mechanical deformation) of RBCs and subsequently activate mechanosensitive cation channels.⁷⁴ In contrast, some other evidences have suggested that the effect on ATP release of deoxygenation may differ with that of mechanical deformation.^{41, 75} The alternative explanation for the hypoxia-induced ATP release is that deoxygenation on RBC may disrupt the protein complexes within spectrin-actin cytoskeleton of its membranes.⁷⁶ In the present study, we sought to further identify the underlying mechanisms of the hypoxia-induced impairment of RBC deformability from the perspective of molecular basis. The impairment of RBC deformability in response to low oxygen tension can be presumably attributed to the mechanisms of hypoxia-induced intracellular ATP release as well as the associated cation transport, e.g. influx of Ca^{2+} .^{5, 14, 75} Our results confirm such speculation by observation of the elevated intracellular Ca^{2+} content in RBCs after cyclic hypoxia. However, inhibition of the mechanosensitive cation channels did not show any effect on the repeated deoxygenation-induced mechanical degradation of RBCs, suggesting that the hypoxia-induced and deformation-induced fatigue failure of RBC might underly different mechanisms. Alternatively, we found kinase-regulated phosphorylation and downstream damage in the spectrin-actin cytoskeleton might entail mechanical degradation in RBC membranes under the challenge of cyclic hypoxia. In addition, the cyclic hypoxic effect on sickle RBCs is more complicated compared to normal RBCs, because sickle RBCs simultaneously undergo drastic mechanical deformation (localized membrane crenation) during the sickling/unsickling process.⁷⁴ This might be an important reason for why sickle cells have more tendency of mechanical degradation under cyclic hypoxia and shortened lifespan compared to healthy RBCs.

RBC was selected for the single-cell investigation tested on the system developed here mainly for three reasons: (1) Due to the absence of a nucleus and of a complex 3D cytoskeleton in the disk-shaped RBC facilitates relatively easier analyses of its deformation; (2) RBC is most common type of biological cells that is responsible for oxygen transport in human body; (3) As RBCs are subjected to intermittent shear stress as well as oxidative stress during the blood circulation, deformability under the influence of oxygen tension variations is an essential feature of RBCs. Due to the limitations in throughput and long-duration of experiments, we need to be very careful about the interpretation of our results

especially on the molecular pathways associated with cyclic hypoxia on RBCs. Therefore, we mainly focused on the mechanical degradation of RBCs, and only explored a couple of known pathways that might play a role during cyclic hypoxia. We especially examined the differences between non-cyclic hypoxia vs cyclic hypoxia and documented any cumulative effect vs hypoxia cycles, i.e. aspects that have not been studied quantitatively in the literature. RBC deformability is an important biomarker of its functionality. Mechanical properties measured here, i.e., shear modulus (μ) and shear viscosity (η), are associated with cell deformability and can determine whether RBCs can pass through the smallest openings in circulation (i.e., the smallest capillaries and spleen). Therefore, these measurements could provide important computational parameters for the modeling/prediction of RBC passage through inter-endothelial slits.^{77, 78}

We anticipate this system can be used as a mechanical characterization tool for other cell types involved in oxygen-dependent biological processes. For instance, cancer cells are more metastatic in a hypoxic tumor microenvironment,⁷⁹ and cancer cell stiffness was shown to be an effective biomarker of their metastatic potential.^{80, 81} In fact, a certain number of similar electrodeformation platforms have been engineered to perform mechanical testing of other types of cells, such as MCF-7 cells, MDA-MB-231 cells and NB4 cells.^{82, 83} However, to our knowledge, none of these existing studies have involved the hypoxic effect due to the limitation of their assays. In this light, we envision the developed microfluidic assay in the present study holds the promise for investigation of hypoxic effects on metastatic potential and relevant drug resistance of cancer cells. The presented device in the current form is merely suitable for the measurement of floating cells, however, it still can be employed to measure the mechanical properties of adherent cells while they are shortly detached from the substrate. Besides, this method could be further accommodated for the purpose of testing adherent cells by means of appropriate modification in the device configurations.⁸⁴

Conclusions

The developed microfluidic assay for probing the mechanical performance of RBCs is multifaceted. It provides a well-controlled cyclic loading of separate and simultaneous shear and oxidative stressing to cells in suspension, allowing characterization of individual RBC deformability and membrane viscoelasticity as cellular biophysical markers of therapeutic treatments. This work demonstrated that the cyclic oxidative stressing (DeOxy-Oxy challenge) is a separate mechanism, acting simultaneously with the cyclic shear loading in RBCs, leading to the fatigue failure in cell membranes during blood circulation. We further demonstrated that impairment effect on RBC deformability under hypoxic condition is cumulative, and depending on the loading occasions, oxygen tension levels, and cell pathological states such as in sickle cell disease. The mechanism underlying deoxygenation-induced impairment of RBC deformability was investigated by inhibiting part of signalling pathways of RBCs. It was further manifested by modification of both normal and sickle RBCs using 5-HMF, which improves oxygen affinity of hemoglobin and the mechanical performance of cells. We envision this method can be a useful tool to predict the mechanical performance of natural and artificial RBCs for transfusion purposes as well as to assess the efficacy of relevant reagents in extending cellular lifespan in circulation. Measurements of biomarkers, such as oxidative damage and ATP release can provide additional information to

establish quantitative relationships between the fatigue loading and the biological processes, allowing us to better understand the RBC failure and senescence. The microfluidic assay can also be extended to study other types of biological cells for their mechanical performance and response to gaseous environment.

Supplementary Material

Refer to Web version on PubMed Central for supplementary material.

Acknowledgements

This material is based upon work supported by the National Science Foundation under Grant No. 1635312 and 1941655. YQ and MD acknowledge support by the National Institutes of Health under Grant No. R01HL158102 and R01HL154150. The authors thank Dr. Ofelia Alvarez, M.D., at the Division of Pediatric Hematology and Oncology, University of Miami, and Dr. John Higgins, M.D., at Massachusetts General Hospital, for providing the sickle cell samples.

References

1. Eales K, Hollinshead K and Tennant D, *Oncogenesis*, 2016, 5, e190–e190. [PubMed: 26807645]
2. Lenihan Colin R. and Taylor Cormac T., *Biochemical Society Transactions*, 2013, 41, 657–663. [PubMed: 23514172]
3. Hung SP, Ho JH, Shih YRV, Lo T and Lee OK, *Journal of Orthopaedic Research*, 2012, 30, 260–266. [PubMed: 21809383]
4. Brennan MD, Rexius-Hall ML, Elgass LJ and Eddington DT, *Lab on a Chip*, 2014, 14, 4305–4318. [PubMed: 25251498]
5. Grygorczyk R and Orlov SN, *Frontiers in physiology*, 2017, 8, 1110. [PubMed: 29312010]
6. Mohanty JG, Nagababu E and Rifkind JM, *Frontiers in physiology*, 2014, 5, 84–84. [PubMed: 24616707]
7. McNamee AP, Horobin JT, Tansley GD and Simmonds MJ, *Artificial organs*, 2018, 42, 184–192. [PubMed: 28877350]
8. Doyle MP and Walker BR, *Journal of applied physiology*, 1990, 69, 1270–1275. [PubMed: 2124584]
9. Tuvia S, Levin S and Korenstein R, *Biophysical journal*, 1992, 63, 599–602. [PubMed: 1420901]
10. Uyklu M, Meiselman HJ and Baskurt OK, *Clinical hemorheology and microcirculation*, 2009, 41, 179–188. [PubMed: 19276515]
11. Kaniewski W, Hakim T and Freedman J, *Biorheology*, 1994, 31, 91–101. [PubMed: 8173047]
12. George A, Pushkaran S and Konstantinidis DG, *Blood*, 2014, 123, 1972–1972.
13. Mackie LH and Hochmuth RM, *Blood*, 1990, 76, 1256–1261. [PubMed: 2400812]
14. Racine ML and Dinunno FA, *The Journal of physiology*, 2019, 597, 4503–4519. [PubMed: 31310005]
15. Presley TD, Perlegas AS, Bain LE, Ballas SK, Nichols JS, Sabio H, Gladwin MT, Kato GJ and Kim-Shapiro DB, *Hemoglobin*, 2010, 34, 24–36. [PubMed: 20113285]
16. Padilla F, Bromberg P and Jensen W, *Blood*, 1973, 41, 653–660. [PubMed: 4694082]
17. Bessis M, Feo C and Jones E, *Blood Cells*, 1982, 8, 17–28. [PubMed: 7115975]
18. Qiang Y, Liu J, Dao M, Suresh S and Du E, *Proceedings of the National Academy of Sciences*, 2019, DOI: 10.1073/pnas.1910336116,201910336.
19. Qiang Y, Liu J and Du E, *Acta biomaterialia*, 2017, 57, 352–362. [PubMed: 28526627]
20. Tomaiuolo G, *Biomicrofluidics*, 2014, 8, 051501. [PubMed: 25332724]
21. Sinha A, Chu TT, Dao M and Chandramohanadas R, *Scientific reports*, 2015, 5, 1–8.
22. Low P, Waugh S, Zinke K and Drenckhahn D, *Science*, 1985, 227, 531–533. [PubMed: 2578228]

23. Huisjes R, Bogdanova A, van Solinge WW, Schiffelers RM, Kaestner L and Van Wijk R, *Frontiers in physiology*, 2018, 9, 656. [PubMed: 29910743]
24. Boivin P, *Biochem. J.*, 1988, 256, 689–695. [PubMed: 3066352]
25. Kuck L, Peart JN and Simmonds MJ, *Biochim. Biophys. Acta, Mol. Cell Res.*, 2020, 1867, 118802. [PubMed: 32717279]
26. Tiffert T, Etzion Z, Bookchin R and Lew V, *The Journal of physiology*, 1993, 464, 529–544. [PubMed: 8229816]
27. Moura PL, Lizarralde Iragorri MA, Français O, Le Pioufle B, Dobbe JGG, Streekstra GJ, El Nemer W, Toye AM and Satchwell TJ, *Blood Adv*, 2019, 3, 2653–2663. [PubMed: 31506283]
28. Brunati AM, Bordin L, Clari G, James P, Quadroni M, Baritono E, Pinna LA and Donella-Deana AJB, *The Journal of the American Society of Hematology*, 2000, 96, 1550–1557.
29. Franco T and Low PS, *Transfusion clinique et biologique*, 2010, 17, 87–94. [PubMed: 20655268]
30. Marzocchi B, Ciccoli L, Tani C, Leoncini S, Rossi V, Bini L, Perrone S and Buonocore G, *Pediatr. Res.*, 2005, 58, 660–665. [PubMed: 16189190]
31. Barbul A, Zipser Y, Nachles A and Korenstein RJ, *FEBS Lett.*, 1999, 455, 87–91. [PubMed: 10428478]
32. Nash GB, Johnson CS and Meiselman HJ, *Blood*, 1988, 72, 539–545. [PubMed: 3401593]
33. Itoh T, Chien S and Usami S, *Blood*, 1995, 85, 2245–2253. [PubMed: 7718897]
34. Seo S, Mastiani M, Hafez M, Kunkel G, Asfour CG, Garcia-Ocampo KI, Linares N, Saldana C, Yang K and Kim M, *International Journal of Greenhouse Gas Control*, 2019, 83, 256–264.
35. Lamberti A, Marasso S and Cocuzza M, *Rsc Advances*, 2014, 4, 61415–61419.
36. Lam SF, Shirure VS, Chu YE, Soetikno AG and George SC, *PLoS One*, 2018, 13, e0209574. [PubMed: 30571786]
37. Abbyad P, Tharoux P-L, Martin J-L, Baroud CN and Alexandrou A, *Lab on a Chip*, 2010, 10, 2505–2512. [PubMed: 20603684]
38. Du E and Dao M, *Experimental mechanics*, 2019, 59, 319–325. [PubMed: 31178599]
39. Lee I, Woo JH, Lee M, Jeon T-J and Kim SM, *Micromachines*, 2019, 10, 16.
40. Zheng Y, Cachia MA, Ge J, Xu Z, Wang C and Sun Y, *Lab on a Chip*, 2015, 15, 3138–3146. [PubMed: 26066022]
41. Zhou S, Giannetto M, DeCoursey J, Kang H, Kang N, Li Y, Zheng S, Zhao H, Simmons WR, Wei HS and Bodine DM, *Sci. Adv.*, 2019, 5, eaaw4466. [PubMed: 31149638]
42. Man Y, Kucukal E, An R, Watson QD, Bosch J, Zimmerman PA, Little JA and Gurkan UA, *Lab Chip*, 2020, 20, 2086–2099. [PubMed: 32427268]
43. Lu X, Chaudhury A, Higgins JM and Wood DK, *Am. J. Hematol.*, 2018, 93, 1227–1235. [PubMed: 30033564]
44. Carlo DD and Lee LP, *Anal. Chem.*, 2006, 78, 7918–7925. [PubMed: 17186633]
45. Kim J, Lee H and Shin S, *Journal of Cellular Biotechnology*, 2015, 1, 63–79.
46. Zhang H and Liu K-K, *Journal of The Royal Society Interface*, 2008, 5, 671–690.
47. Brecher G and Schneiderman M, *Am. J. Clin. Pathol.*, 1950, 20, 1079–1083. [PubMed: 14783090]
48. Heo YS, Cabrera LM, Song JW, Futai N, Tung Y-C, Smith GD and Takayama S, *Anal. Chem.*, 2007, 79, 1126–1134. [PubMed: 17263345]
49. Du E, Dao M and Suresh S, *Extreme Mechanics Letters*, 2014, 1, 35–41. [PubMed: 26029737]
50. Hochmuth R and Waugh R, *Annual review of physiology*, 1987, 49, 209–219.
51. Qiang Y, Liu J and Du E, *Micromachines*, 2018, 9, 21. [PubMed: 29682335]
52. Hertz L, Huisjes R, Llaudet-Planas E, Petkova-Kirova P, Makhro A, Danielczok JG, Egee S, del Mar Mañú-Pereira M, Van Wijk R, Vives Corrons JL and Bogdanova A, *Frontiers in Physiology*, 2017, 8, 673. [PubMed: 28932200]
53. Gnanasambandam R, Ghatak C, Yasman A, Nishizawa K, Sachs F, Ladokhin AS, Sukharev SI and Suchyna TM, *Biophys. J.*, 2017, 112, 31–45. [PubMed: 28076814]
54. Gascoyne P, Mahidol C, Ruchirawat M, Satayavivad J, Watcharasit P and Becker FF, *Lab on a Chip*, 2002, 2, 70–75. [PubMed: 15100837]
55. Mills J, Qie L, Dao M, Lim C and Suresh S, *MCB-TECH SCIENCE PRESS-*, 2004, 1, 169–180.

56. LaCelle PL and Weed RI, *J. Clin. Invest*, 1970, 49, A54.
57. Cinar E, Zhou S, DeCoursey J, Wang Y, Waugh RE and Wan J, *Proceedings of the National Academy of Sciences of the United States of America*, 2015, 112, 11783–11788. [PubMed: 26351678]
58. Saldanha C, Silva AS, Gonçalves S and Martins-Silva J, *Clin. Hemorheol. Microcirc*, 2007, 36, 183–194. [PubMed: 17361021]
59. Kaul DK, Fabry M, Windisch P, Baez S and Nagel R, *The Journal of clinical investigation*, 1983, 72, 22–31. [PubMed: 6874947]
60. Itoh T, Chien S and Usami S, *Blood*, 1992, 79, 2141–2147. [PubMed: 1562740]
61. Celle P, *Transfusion*, 1969, 9, 238–245. [PubMed: 5822775]
62. Hebbel R, *Blood*, 1991, 77, 214–237. [PubMed: 1985689]
63. Evans E, Mohandas N and Leung A, *The Journal of clinical investigation*, 1984, 73, 477–488. [PubMed: 6699172]
64. Zhao L, Chen J, Su J, Li L, Hu S, Li B, Zhang X, Xu Z and Chen T, *Journal of agricultural and food chemistry*, 2013, 61, 10604–10611. [PubMed: 24107143]
65. Abdulmalik O, Safo MK, Chen Q, Yang J, Brugnara C, Ohene-Frempong K, Abraham DJ and Asakura T, *British journal of haematology*, 2005, 128, 552–561. [PubMed: 15686467]
66. Hannemann A, Cytlak UM, Rees DC, Tewari S and Gibson JS, *The Journal of physiology*, 2014, 592, 4039–4049. [PubMed: 25015917]
67. Vichinsky E, Hoppe CC, Ataga KI, Ware RE, Nduba V, El-Beshlawy A, Hassab H, Achebe MM, Alkindi S, Brown RC, Diuguid DL and Telfer P, *N. Engl. J. Med*, 2019, 381, 509–519. [PubMed: 31199090]
68. Demirci S, Leonard A, Haro-Mora JJ, Uchida N and Tisdale JF, in *Cell Biology and Translational Medicine, Volume 5: Stem Cells: Translational Science to Therapy*, ed. Turksen K, Springer International Publishing, Cham, 2019, DOI: 10.1007/5584_2018_331, pp. 37–52.
69. Wei HS, Kang H, Rasheed I-YD, Zhou S, Lou N, Gershteyn A, McConnell ED, Wang Y, Richardson KE, Palmer AF, Xu C, Wan J and Nedergaard M, *Neuron*, 2016, 91, 851–862. [PubMed: 27499087]
70. Bergfeld GR and Forrester T, *Cardiovasc Res*, 1992, 26, 40–47. [PubMed: 1325292]
71. Chang SH and Low PS, *J. Biol. Chem*, 2001, 276, 22223–22230. [PubMed: 11294862]
72. Grau M, Lauten A, Hoepfner S, Goebel B, Brenig J, Jung C, Bloch W and Suhr F, *Clin. Hemorheol. Microcirc*, 2016, 63, 199–215. [PubMed: 26890238]
73. Forsyth AM, Wan J, Owrutsky PD, Abkarian M and Stone HA, *Proceedings of the National Academy of Sciences of the United States of America*, 2011, 108, 10986–10991. [PubMed: 21690355]
74. Park Y, Best CA, Auth T, Gov NS, Safran SA, Popescu G, Suresh S and Feld MS, *Proc. Natl. Acad. Sci. U. S. A.*, 2010, 107, 1289–1294. [PubMed: 20080583]
75. Faris A and Spence DM, *Analyst*, 2008, 133, 678–682. [PubMed: 18427692]
76. Mohandas N and Gallagher PG, *Blood*, 2008, 112, 3939–3948. [PubMed: 18988878]
77. Freund JB, *Phys. Fluids*, 2013, 25, 110807.
78. Pivkin IV, Peng Z, Karniadakis GE, Buffet PA, Dao M and Suresh S, *Proceedings of the National Academy of Sciences of the United States of America*, 2016, 113, 7804–7809. [PubMed: 27354532]
79. Osinsky S, Zavelevich M and Vaupel P, *Exp Oncol*, 2009, 31, 80–86. [PubMed: 19550396]
80. Xu W, Mezencev R, Kim B, Wang L, McDonald J and Sulchek T, *PLoS One*, 2012, 7, e46609. [PubMed: 23056368]
81. Swaminathan V, Mythreye K, O'Brien ET, Berchuck A, Blobe GC and Superfine R, *Cancer research*, 2011, 71, 5075–5080. [PubMed: 21642375]
82. Teng Y, Pang M, Huang J and Xiong C, *Sensors and Actuators B: Chemical*, 2017, 240, 158–167.
83. Bai G, Li Y, Chu HK, Wang K, Tan Q, Xiong J and Sun D, *Biomedical engineering online*, 2017, 16, 41. [PubMed: 28376803]
84. Urbano RL and Clyne AM, *Lab on a Chip*, 2016, 16, 561–573. [PubMed: 26738543]

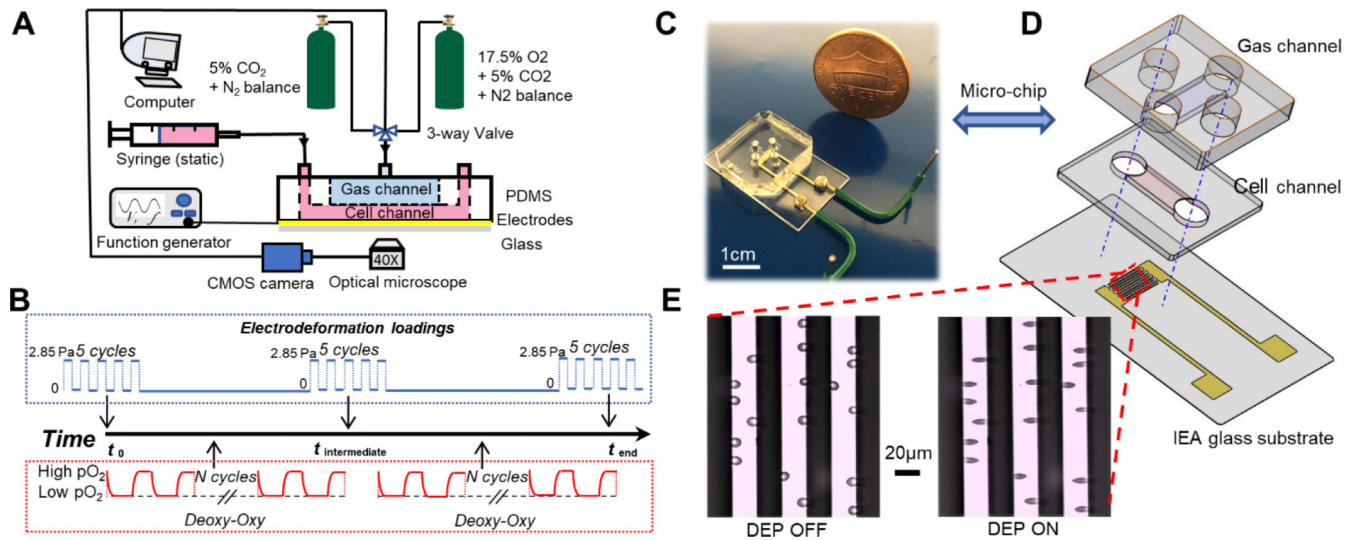


Fig. 1. Microfluidics-based biomechanical assay with controlled oxygen tension environment. (A) A schematic of the experimental setup. (B) Timeline of the mechanical measurements of RBCs along the DeOxy-Oxy cycling. (C) The microfluidic chip for electro-deformation of single cells in suspension. (D) Exploded view drawing of the microfluidic chip. (E) Microscopic images of RBCs in free suspension when DEP field was OFF (left) and being trapped and elongated when DEP field was ON (right).

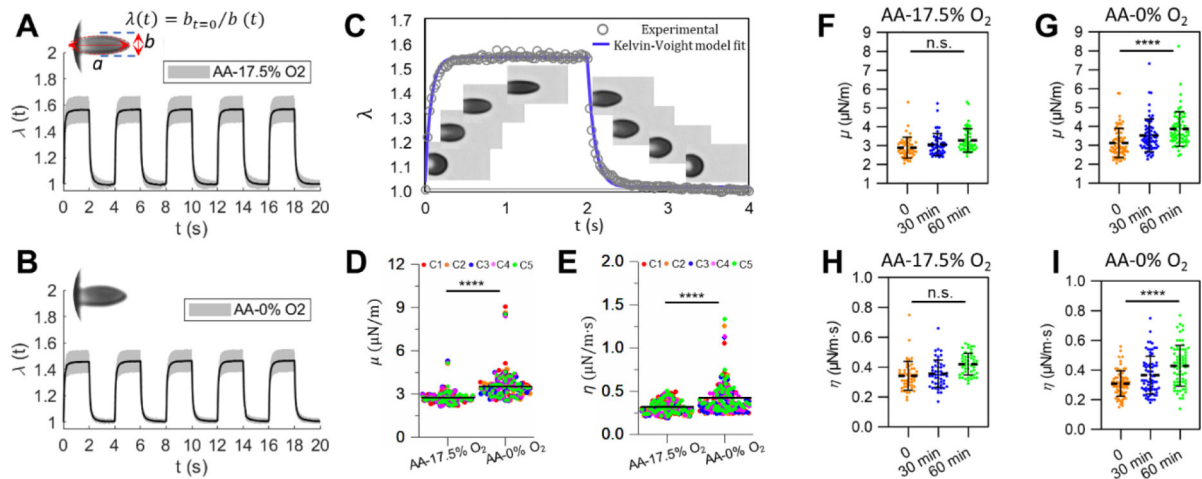
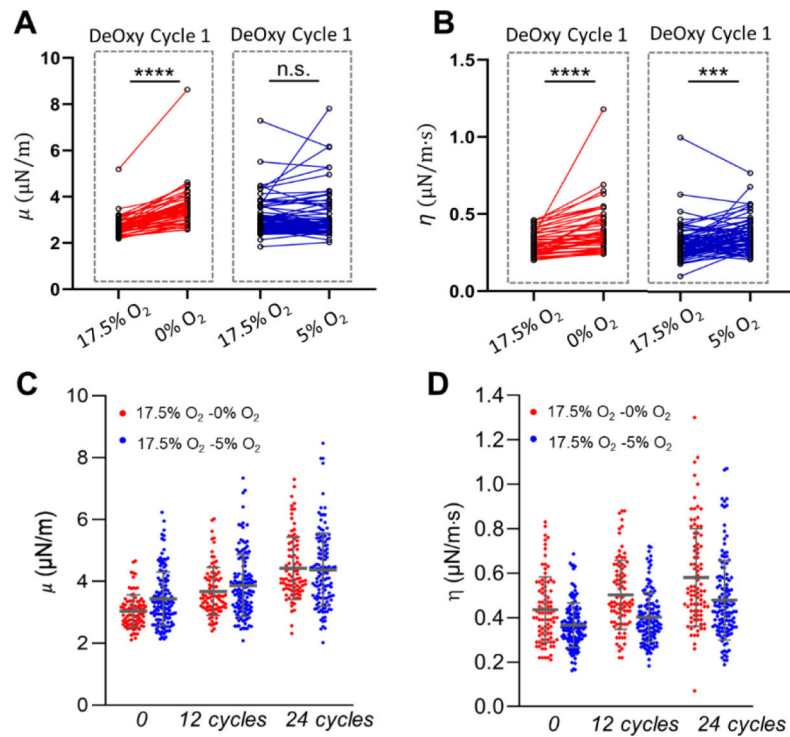
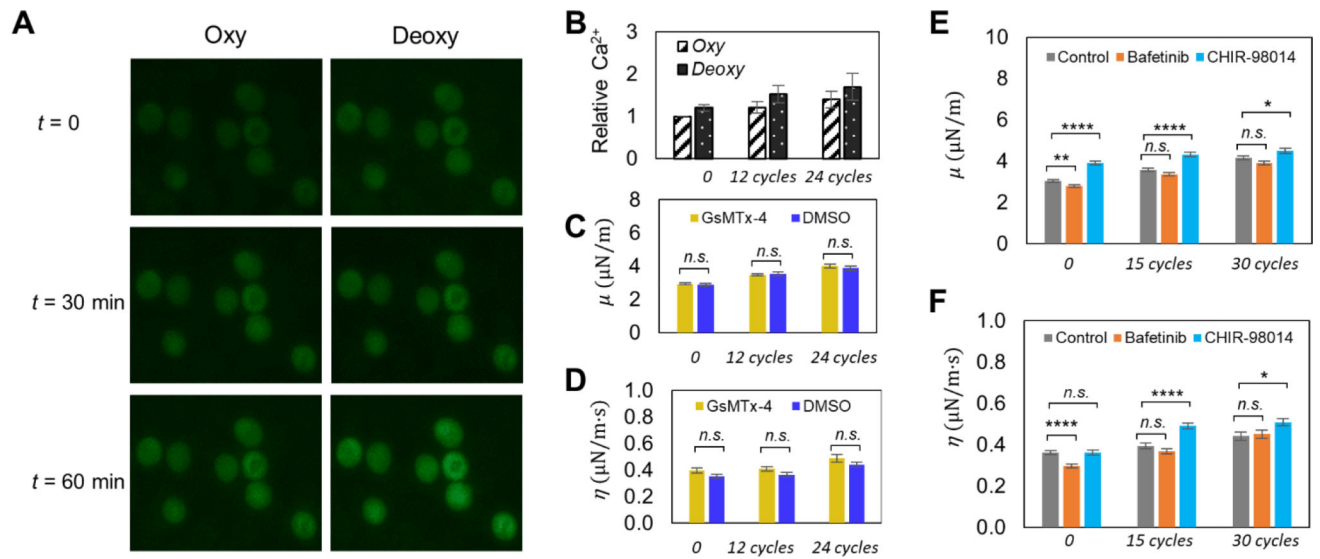


Fig. 2.

Deformability of normal RBCs (AA) measured under different static (i.e. non-cyclic) oxygen conditions. (A and B) Instantaneous values of λ averaged from individually tracked cells in the 5 continuous cycles of mechanical testing. Insets show representative images of deformed cells. (C) Experimental data of viscoelastic deformation for a representative RBC, fitted to the Kelvin-Voigt model. Insets are time sequences of microscopic images of a representative RBC. (D and E) Comparisons of the corresponding values of μ and η of normal RBCs under 17.5% O_2 and 0% O_2 . Each symbol represents a single cell measurement. Each color of the data points represents a different measurement cycle in the 5 cycles (C1-C5). (F and H) Changes in the values of μ and η of normal RBCs under 17.5% O_2 lasting for 1 hour. (G and I) Changes in the values of μ and η of normal RBCs under 0% O_2 lasting for 60 min. * $p < 0.05$, ** $p < 0.01$, *** $p < 0.001$, **** $p < 0.0001$, n.s., not significant.

**Fig. 3.**

The influence of oxygen conditions on the RBC deformability for the same individual RBCs. (A and B) Longitudinal tracking of the changes in shear modulus μ and shear viscosity η after a single DeOxy switch between different oxygen levels 17.5% O_2 vs 0% O_2 and 17.5% O_2 vs 5% O_2 , respectively. (C and D) Comparison of the progression of μ and η values between two different cyclic deoxygenation conditions: 17.5% O_2 - 5% O_2 and 17.5% O_2 - 0% O_2 . * $p < 0.05$, ** $p < 0.01$, *** $p < 0.001$, **** $p < 0.0001$, n.s., not significant.

**Fig. 4.**

(A) Influence of intracellular Ca^{2+} content on the deformability change of RBCs under cyclic loadings of deoxygenation-oxygenation (DeOxy-Oxy). Representative fluorescence images of Fluo-4 loaded RBCs under oxygenation and deoxygenation at different time points during the cyclic DeOxy-Oxy loadings. (B) Comparisons of relative intracellular Ca^{2+} concentration between oxygenated and deoxygenated RBCs at different time points. (C and D) Comparison of changes in the values of μ and η of normal RBCs between of GsMTx-4 incubated samples and DMSO control samples. (E and F) Comparison of changes in the values of μ and η of normal RBCs between of Bafetinib and CHIR-98014 incubated samples and DMSO control samples. * $p < 0.05$, ** $p < 0.01$, *** $p < 0.001$, **** $p < 0.0001$, n.s., not significant.

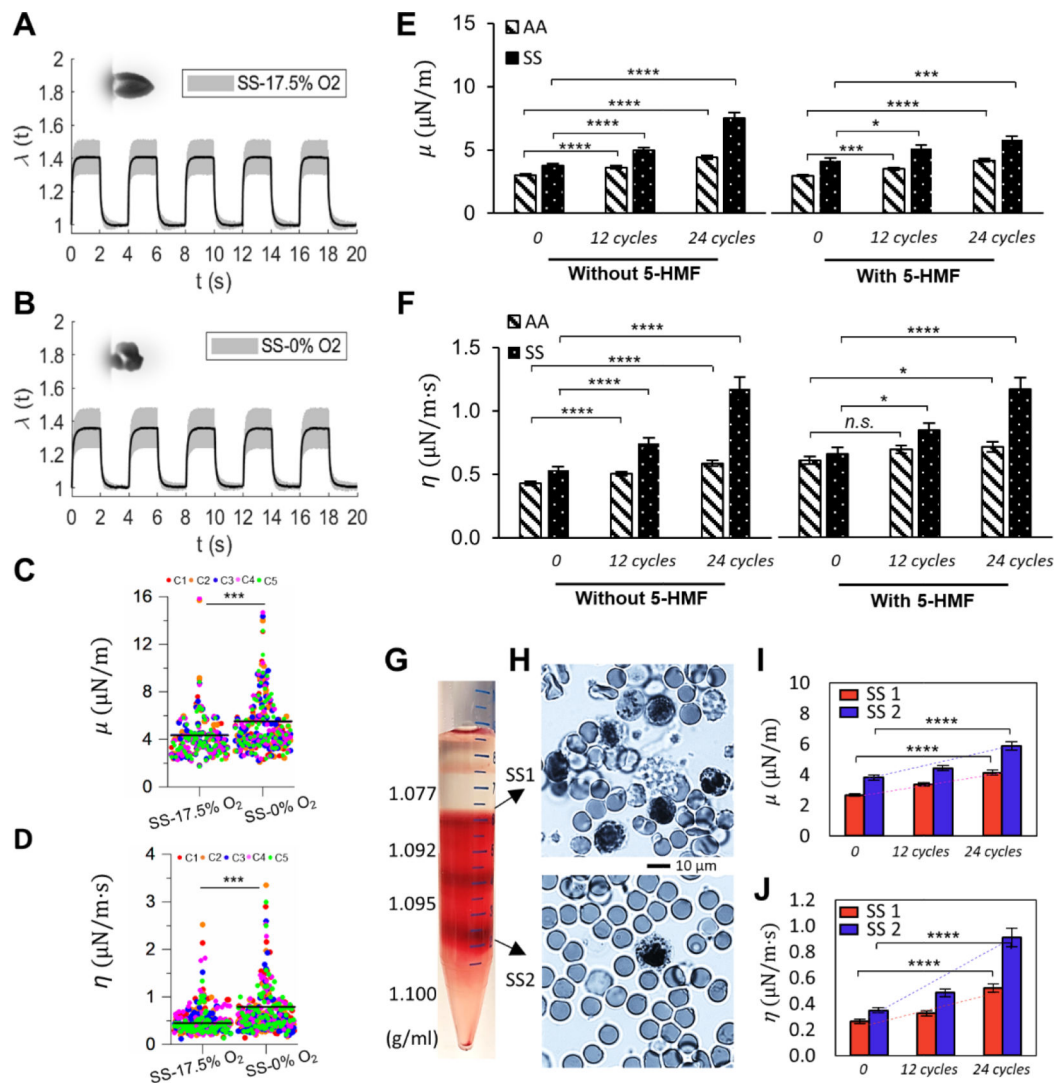


Fig. 5. Deformability of sickle RBCs (SS) measured under different oxygen conditions. (A and B) Instantaneous values of λ averaged from individually tracked SS cells in the 5 continuous cycles of mechanical testing. Insets show representative images of deformed SS RBCs. (C and D) Comparisons of the corresponding values of μ , and η of normal RBCs under 17.5% O_2 and 0% O_2 . Each symbol represents a single cell measurement. Each color of the data points represents a different measurement cycle in the 5 cycles (C1-C5). (E and F) Comparison of changes in the values of μ and η of AA RBCs and SS RBCs under cyclic DeOxy-Oxy (120s-30s). Data is measured at $N=0$ cycle, 12 cycles and 24 cycles. Further comparisons were carried out between samples with treatment and without treatment of 5-HMF. (G) Density separation of RBCs from SCD patients by different cell density fractions of 1.077, 1.092, 1.095 and 1.100 g/mL. (H) Blood smears stained with methylene blue of the reticulocyte-rich (SS1) and erythrocyte-rich (SS2) cell subpopulations. (I and J) Comparison of changes in the values of μ and η of RBCs from SS1 and SS2 sub-populations

under cyclic DeOxy-Oxy. * $p < 0.05$, ** $p < 0.01$, *** $p < 0.001$, **** $p < 0.001$, n.s, not significant. Normal RBCs – AA; Sickle RBCs – SS.

Author Manuscript

Author Manuscript

Author Manuscript

Author Manuscript